ACS Macro Letters

pubs.acs.org/macroletters Letter

Phase Transition of Catenated DNA Networks in Poly(ethylene glycol) Solutions

Indresh Yadav,[‡] Dana Al Sulaiman,[‡] Beatrice W. Soh, and Patrick S. Doyle*

Cite This: ACS Macro Lett. 2021, 10, 1429−1435 Read Online

ACCESS | Metrics & More | Article Recommendations | Supporting Information

ABSTRACT: Conformational phase transitions of macromolecules are an important class of problems in fundamental polymer physics. While the conformational phase transitions of linear DNA have been extensively studied, this feature of topologically complex DNA remains unexplored. We report herein the polymer-and-salt-induced (Ψ) phase transition of 2D catenated DNA networks, called kinetoplasts, using single-molecule fluorescence microscopy. We observe that kinetoplasts can undergo a reversible transition from the flat phase to the collapsed phase in the presence of NaCl as a function of the crowding agent poly(ethylene glycol). The nature of this phase transition is tunable through varying ionic strengths. For linear DNA, the coexistence of coil and globule phases was attributed to a first order phase transition associated with a double well potential in the transition regime. Kinetoplasts, however, navigate from the flat to the collapsed phase by passing through an intermediate regime, characterized by the coexistence of a multipopulation with varying shapes and sizes. Conformations of individual molecules in the multipopulation are long-lived, which suggests a rugged energy landscape.

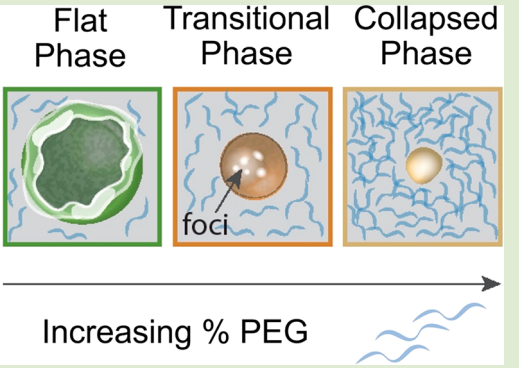

Studying the relationship between molecular topology and functional behavior is a longstanding area of importance in polymer physics.[1−5] In this regard, linear polymers and their derivatives (e.g., rings, stars, ladders, knots, and 3D networks) have been extensively investigated.[6] However, polymers that would form molecular objects of a well-defined shape (e.g., rods, molecular tubes, and sheets) show significant departure from the linear chain and its derivatives.[7] The synthesis and understanding of the physical behavior of these objects are the subject of contemporary polymer science.[8−12] Tuning and controlling the topological constraints plays a vital role in such systems. In particular, a system of several rings can display a variety of topological states, including the formation of catenane with varying degrees of catenation.[13−15] One example of a natural catenated polymeric system is a kinetoplast.[16,17]

A single kinetoplast (kDNA) molecule from trypanosomatid *Crithidia fasciculata* is a planar network of approximately 5000 minicircles (∼2.5 kbp) and 25 maxicircles (∼40 kbp).[18] Each minicircle is on average topologically linked to three other minicircles.[18,19] The much larger maxicircles are topologically linked by threading through the minicircles, forming a network within a network.[17] A simplified structure of a kinetoplast is presented in Figure 1a. The lateral percolation of catenation in kinetoplasts makes them an example of 2D polymers.[20] Though topologically planar, the kinetoplast is an Olympic gel.[21] Recently, our group has proposed kinetoplasts as a model system for studying the physical behavior of catenated polymers.[22−26]

Understanding such a catenated system can advance our knowledge of 2D polymers. A 2D polymer is a single-layered polymer that forms a tiling network in two dimensions.[7,20] Many recent efforts have been directed toward developing and advancing the synthesis of 2D polymers;[27] however, experimental studies investigating their physical behavior are limited. Despite their crucial applications,[28] the conformational behavior of 2D polymers remains a controversial issue in literature. For example, while the existence of crumpled and collapsed phases of 2D polymers was predicted three decades ago,[29,30] experimental results are still inconclusive. Static light scattering performed on graphite oxide showed the existence of a crumpled phase in good solvents and a collapsed phase in poor solvents.[31] However, a consensus has not yet been reached.[32,33]

A recent study showed that rich conformal phases can be obtained by tuning intramolecular interactions.[34] In dilute solutions, the conformation of polymer molecules is governed by the interplay of configurational entropy and intramolecular interactions that can be tuned by varying the solvent quality. This feature plays a crucial role in many domains, including

Received: July 14, 2021
Accepted: November 2, 2021

https://doi.org/10.1021/acsmacrolett.1c00463
ACS Macro Lett. 2021, 10, 1429−1435

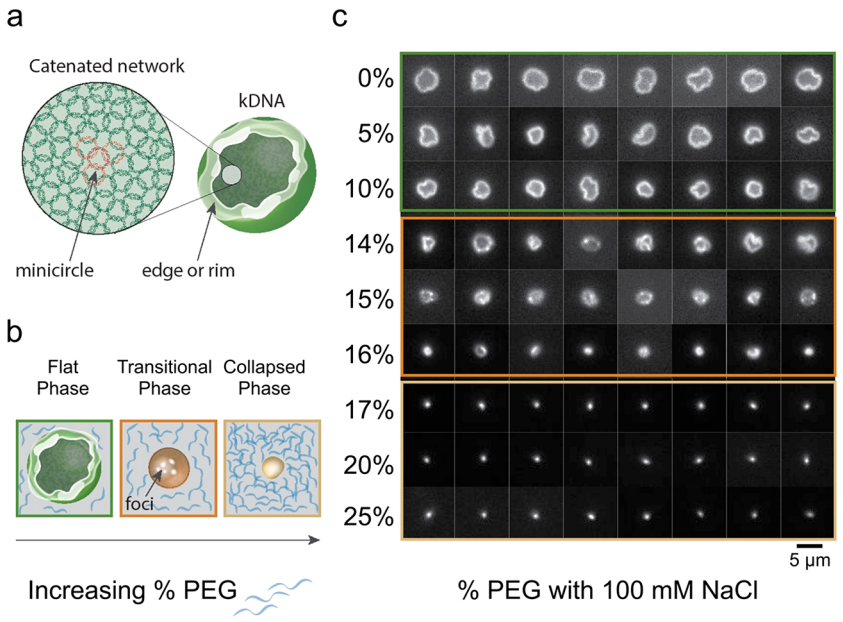

Figure 1. Internal structure of a kinetoplast and its transition from flat phase to collapsed phase. (a) Schematic diagram of a kinetoplast, a catenated 2D structure made of thousands of connected rings of circular DNA. Under good solvent conditions the kinetoplast shape can be described as a wrinkled bowl with a bright edge or rim. The zoomed-in image shows the connectivity of minicircles with an average catenation valency of three[45] (maxicircles that represent <0.1% of the total network mass have not been shown for simplicity). (b) Schematic diagram representing three phases of a kinetoplast in the presence of NaCl salt with increasing concentrations of PEG (% wt/vol). (c) Fluorescence images of different kinetoplasts inside a 2 μm tall channel showing a gradual decrease in size with increasing PEG concentration in the presence of 100 mM NaCl. Molecules navigate from flat (0−10% PEG) to collapsed phase (17−25% PEG) by passing through a transition regime (14−16% PEG).

medicine, molecular biology, and materials science. For example, nanopore-based DNA sequencing depends on the speed of DNA translocations that can be controlled by tuning solvent quality.[35] It has been shown that DNA molecules can be spontaneously collapsed by excluded volume interactions in solutions containing sufficient concentrations of neutral polymers and salts.[36−40] Polymer-and-salt-induced (Ψ) condensation of linear DNA has greatly contributed to the understanding of the conformal behavior of linear polymers in theta and poor solvents and to the packing of DNA in vivo.[41] Despite its fundamental importance in biology and materials science, Ψ-condensation of ring and catenated polymers has not yet been explored. Direct observations of single molecules to study such phase transitions would be beneficial. Combining fluorescence microscopy with microfluidic channels presents an ideal platform for such experiments.[42] In this Letter, we report the Ψ-phase transition of kinetoplasts using poly(ethylene glycol) (PEG) as the crowding polymer in the presence of NaCl inside microfluidic channels.

Experiments were conducted in straight channels with a 2 μm height, 40 μm width, and 1 cm length. Our prior work shows that this channel height orients kinetoplasts for ease of imaging and only moderately confines the molecules.[22] kDNA from *Crithidia fasciculata* (TopoGEN) was stained with YOYO-1 fluorescent dye at a base pair to dye ratio of 8:1 and allowed to equilibrate overnight at 4 °C. Stock solutions and samples were prepared in 0.5× tris-boric acid-ethylenediaminetetraacetic acid (TBE) buffer. See Supporting Information (SI) for additional experimental details.

A montage of fluorescence images of kinetoplasts inside a 2 μm tall microfluidic channel in the presence of 100 mM NaCl with varying concentrations of PEG (MW 10000 Da) is shown in Figure 1c. The image represents a single frame (frame number 137, chosen arbitrarily) out of 1000 frames recorded for each kinetoplast. Each row displays the typical shape and size variability of molecules at a fixed concentration of PEG from which we can infer the following qualitative information. At low concentration (up to 10% wt./vol) of PEG, all the molecules have a nearly elliptical shape, and the outline of the molecules could be clearly identified. The observation of bright edges was attributed to the dense fibril at the periphery of the kinetoplast network.[18] This observation was consistent with previous work from our group.[22,25] These molecules have flat conformation under the nomenclature of 2D polymer physics. On the other hand, at higher concentrations (17−25% wt/vol) of PEG, all the molecules were highly compacted and showed a high degree of uniformity in the intensity distribution. Furthermore, the shape and size of the molecules were highly uniform and appeared to have rotational symmetry and hence belong to the collapsed phase. This depicts the Ψ-phase transition of kinetoplast molecules, which transforms from flat to collapsed phase at higher PEG concentrations in the presence of NaCl. Interesting features can be seen at the intermediate (transition) regime (14−16% wt/vol) of PEG concentration, where molecules appeared neither in the flat nor the collapsed phase. Molecules in this regime contained bright spots on their surface. These spots appeared to increase in size with PEG concentration and become hard to resolve at 16% PEG. The appearance of local bright spots (herein referred to as "local foci") is analogous to the "beads on a string" or "pearl necklace" structure during the coil−globule transition of linear polymers.[43,44] The intricate features of these local foci will be discussed later. A schematic representing typical conformation of the kinetoplast in different regime is presented in Figure 1b.

To have a quantitative evaluation of the kinetoplasts conformation as a function of PEG concentration, we calculated the radius of gyration (R_g) from the 2D projection

https://doi.org/10.1021/acsmacrolett.1c00463
ACS Macro Lett. 2021, 10, 1429−1435

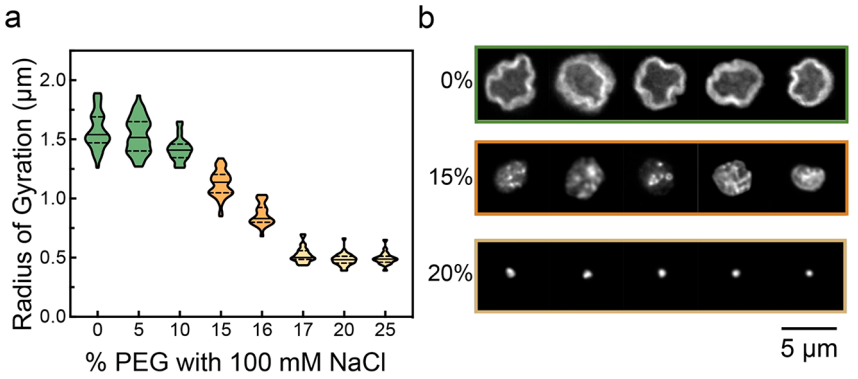

Figure 2. Size distribution of kinetoplasts and confocal microscopy. (a) Violin plots presenting the size (radius of gyration, R_g) distribution of kinetoplasts at varying concentrations of PEG in the presence of 100 mM NaCl. The central solid line shows the median, while the dotted lines represent the ends of the first and third quartiles. The median as a function of PEG concentration decreases gradually, a characteristic of second-order phase transition. (b) Confocal microscopy images of kinetoplasts in the flat phase (0% PEG), transition regime (15% PEG), and in the collapsed phase (20% PEG).

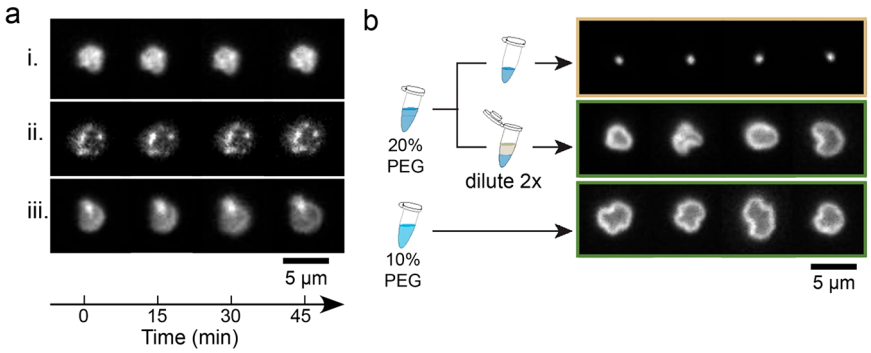

Figure 3. Temporal stability of intermediate structures and reversibility of collapsed phase. (a) Representative kinetoplast molecules in the transition regime (100 mM NaCl, 14% PEG) imaged up to a temporal span of 45 min showing no significant evolution in their appearance. (b) Left panel shows a schematic presenting the experimental procedure to evaluate conformational reversibility after compaction, and corresponding imaged molecules are presented on the right panel.

of the intensity of each kinetoplast. Assuming that the fluorescence intensity is proportional to the mass density of the kinetoplast, R_g maps the kinetoplasts extension in a plane.[26] Here, R_g was determined as the square root of the trace of the radius of gyration tensor.[46] Violin plots representing the distribution of R_g for each PEG concentration are shown in Figure 2a. The width of each violin plot corresponds to the frequency of the data points in each region. The central solid line shows the median, while the dotted lines represent the ends of the first and third quartiles. It can be inferred that the median of R_g decreases gradually with increasing PEG concentration. It saturates, however, at higher PEG concentration. This kind of gradual transition is a signature of second-order phase transitions.[47]

One interesting observation in the microscopy images at transitional PEG concentrations (14−16%) is the appearance of local foci. The appearance and nature of these foci can be better observed through confocal microscopy. Figure 2b depicts confocal images of kinetoplasts in the flat phase (0% PEG), the transition region (15% PEG) and in the collapsed phase (20% PEG). Cup shaped molecules with a clear and bright edge or rim can be seen at 0% PEG, consistent with earlier reports.[22,25] At 15% PEG, the conformation of the molecules is distinct from the flat or collapsed phases, and it is not possible to distinguish a distinct edge or rim around the molecules. Furthermore, the kinetoplasts in this condition are highly heterogeneous, and differences are observed in the number of foci as well as in the location of the foci between individual kinetoplast (see Figure S1 for additional molecules containing local foci). Similar features have been observed using atomic force microscopy in other works that studied kinetoplasts compaction driven by protein-mediated bridging interaction.[48] On the contrary, at 20% PEG, the nature of the molecules is homogeneous. Using confocal microscopy, it became apparent that some molecules were not perfectly symmetrical in shape, and anisotropy can be observed even in the collapsed phase.

Next, we studied the phase stability and reversibility of the kinetoplast (Figure 3). We found that the conformation adopted by individual kinetoplasts in the presence of NaCl and PEG is stable over a long period of time at a given concentration of PEG. A typical example is presented at the intermediate concentration (14% PEG) in Figure 3a. Molecules were imaged up to a temporal span of 45 min with no significant evolution in their size or shape observed. This observation suggests that the structure (local foci) in the transition regime is temporally stable. To investigate the reversibility of the phase transition, we prepared kinetoplasts in 20% PEG solution (100 mM NaCl). We then divided the stock solution into two aliquots. The first aliquot was observed to confirm the collapsed phase. The second aliquot was diluted 2-fold in 0.5× TBE buffer (containing 100 mM NaCl and 4% β-mercaptoethanol) for a final PEG concentration of 10% PEG (Figure 3b). After 2 h, this diluted aliquot was imaged.

https://doi.org/10.1021/acsmacrolett.1c00463
ACS Macro Lett. 2021, 10, 1429−1435

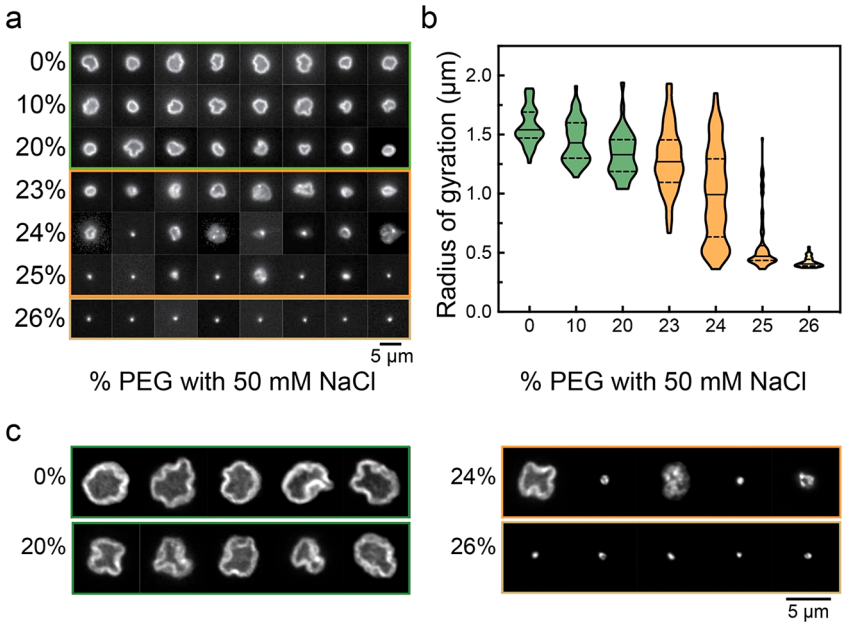

Figure 4. Influence of ionic strength on phase transitions of kinetoplasts. (a) Montage of kinetoplast molecules as a function of PEG concentration in the presence of 50 mM NaCl. Molecules navigate from flat (0−20% PEG) to collapsed phase (26%PEG) by passing through a transition regime (23−25% PEG) characterized by the coexistence of multipopulation. (b) Violin plots presenting the size (radius of gyration) distribution at each concentration of PEG. In the transition regime (23−25% PEG) there is a wide size distribution corresponding to the coexistence of multipopulation. (c) Presents the confocal images of kinetoplasts in the flat phase (0% and 20% PEG), transition regime (24% PEG), and in the collapsed phase (26% PEG).

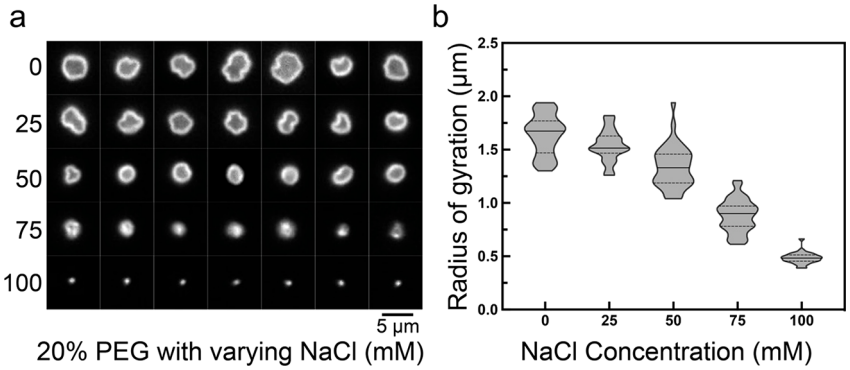

Figure 5. Influence of ionic strength on transition point. (a) Fluorescence images of different kinetoplasts inside a 2 μm tall channel, showing a gradual decrease in size with increasing concentration of NaCl salt at fixed concentration (20% wt/vol) of PEG. (b) Violin plots presenting the size (R_g) distribution of kinetoplasts at varying concentrations of NaCl in the presence of 20% PEG. The median value decreases with increasing concentration of NaCl, indicating that as the intramolecular electrostatic repulsion decreases, entropically driven osmotic force is able to compress individual kinetoplast[58] eventually leading to complete compaction.

Interestingly, the kinetoplasts appeared to be in the flat phase, as expected for kinetoplasts in 10% PEG conditions (100 mM NaCl). A control 10% PEG condition was also prepared and imaged for comparison purposes. No evidence of hysteresis was observed during the phase reversibility. This observation also supports that the cup-like shape (positive Gaussian curvature) of a kinetoplast is its equilibrium conformation in good solvent conditions.[22]

Inspired by the nature of a general phase diagram, we studied the influence of ionic strength on the Ψ-phase transition of kinetoplasts. In particular, we decreased NaCl concentration from 100 to 50 mM. Figure 4a shows a montage of kinetoplast molecules as a function of PEG concentration in the presence of 50 mM NaCl. One notable feature is that kinetoplasts undergo a similar phase transition as in case of 100 mM NaCl, where kinetoplasts transform from the flat to collapsed phase with increasing PEG concentration. However, there are two clear distinctions compared to the 100 mM NaCl condition: (i) the transition point from flat to collapsed phase shifts to higher PEG concentrations and (ii) there is a significantly larger variation in the shape and size of the molecules in the transition regime (23−25% PEG). For quantitative analysis, we calculated the R_g and presented the size distribution using violin plots at each PEG concentration (Figure 4b). Like the system in the presence of 100 mM NaCl, the median values for 50 mM NaCl decreases monotonically with increasing the PEG concentration. However, the size distribution of kinetoplasts at a particular PEG concentration gets broader as it approaches the transition regime, representing wide variability in the sizes. In case of linear DNA, the size distribution in the transition regime was characterized by the bimodal distribution corresponding to the

https://doi.org/10.1021/acsmacrolett.1c00463
ACS Macro Lett. 2021, 10, 1429−1435

coexistence of coil and globule.[49,50] Interestingly and as a notable distinction for kinetoplasts we observed herein the coexistence of multiphases (characterized by continuous and broad size distribution) in the transition regime as shown in the montage of representative molecules in Figure 4a.

To have a better depiction of the morphology of the kinetoplasts, we imaged the molecules using confocal microscopy (Figure 4c). The molecules at 0 and 20% PEG show clear rims and represent the flat phase. On the other hand, at 26% PEG all molecules have a compact and homogeneous structure belonging to the collapsed phase. Interestingly despite the differences in the nature of the phase transition compared to 100 mM NaCl case, the molecules appeared to show local foci at the transition regime (24% PEG), a result indicating that this could be an intrinsic characteristic of the phase transition of 2D catenated polymers. See Figure S2 for additional molecules containing local foci. We also probed the influence of ionic strength at a fixed concentration of PEG (20%), where average size of kinetoplasts decreases with increasing the ionic strength (Figures 5). It shows that the critical value of PEG concentration for phase transition is inversely correlated to the ionic strength. However, the entropically driven osmotic force is not able to drive a phase transition by itself, even at very high PEG concentrations, and screening of the intramolecular electrostatic repulsion is required to facilitate the phase transition. This trend is consistent with Ψ-condensation of linear DNA via PEG where it has been found that a threshold value of added salt is required.[36,38]

Although the intermediate structures show long temporal stability (Figure 3a), the question remains whether these conformations are kinetically arrested or a thermodynamically stable state. To address this question, we generated the intermediate phases (100 mM NaCl, 15% PEG and 50 mM NaCl, 24% PEG) by diluting the system from the collapsed phases (100 mM NaCl, 20% PEG and 50 mM NaCl, 26% PEG) at both salt concentrations, respectively. Data are shown in Figure S3. The molecules prepared in this manner still display the appearance of the local foci, and the overall molecular conformation in the intermediate regime is independent of the direction of the phase transition. This feature, along with long temporal stability (Figure 3a) and continuous phase transition as a function of ionic strength (Figure 5), suggests that the conformation of kinetoplasts with local foci on their surface is a thermodynamically stable state. For comparison, the "beads on a string" conformational state for linear DNA has been reported to be a transient conformation[42,51−53] during chain collapse or a thermodynamically stable[51,54,55] state, depending on the nature of polymer solvent interactions.

The intercalation of YOYO-1 is known to affect the physical properties of DNA.[56,57] Hence, the potential effect of YOYO-1 loading on the nature of phase transition of kinetoplast was investigated. Data examining the phase transition at 50 bp:1 YOYO-1 molecule at 100 mM NaCl and 50 mM NaCl are shown in Figures S4 and S5, respectively. At this staining ratio there is negligible change to the native DNA charge density, twist, and contour length. We find that the nature of the phase transition at this lower staining ratio is similar to that of the 8 bp:1 YOYO-1 complexes. Lowering the staining ratio, however, decreases the critical concentration of PEG at which the phase transition occurs.

For linear DNA the coexistence of coil and globule phases was attributed to a first-order phase transition, associated with a double well potential in the transition regime.[49,50,59,60] However, for kinetoplasts, the coexistence of the multipopulation with varying shapes and sizes (Figures 4 and S2) and long temporal stability (Figure 3a) of the intermediate phases suggest that the energy landscape is rather rugged with multiple local minima. Rugged energy landscapes are a key feature dictating the kinetics of random heteropolymer collapse and protein folding.[61,62] In kinetoplasts, we surmise that the local interactions among rings lead to local foci and ridges which are then frustrated to evolve further via nonlocal interaction that would require bending of the planar structure. While we are unable to follow the collapse kinetics in our current experimental setup, the observed conformations in the multipopulation allow us to speculate that the phase transition from flat-to-collapsed phase does not follow a unique pathway but a multiplicity of routes (a sketch of the postulated routes is presented in Figure S6). Further studies are required to follow the kinetics of the collapse process and better understand the energy landscape for kinetoplast phase transition.

Irrespective of the ionic strength, the interplay of configurational entropy and intramolecular interactions decide the instant conformation of a kinetoplast. With increasing PEG concentration, PEG molecules try to occupy the maximum volume within the system. As a result, PEG imposes an osmotic pressure on kinetoplasts due to excluded volume interactions.[63] Above a threshold concentration of PEG, the entropically driven osmotic pressure wins over the bending rigidity and intramolecular electrostatic repulsions within the kinetoplast, thus, leading the system into the collapsed phase.[58] At higher salt concentration (100 mM NaCl), intramolecular interaction is weak (due to electrostatic screening) and the observed phase transition is continuous, whereas for 50 mM NaCl multiphases coexist. This implies that the ruggedness of energy landscape is inversely correlated to the electrostatic screening. Another interesting observation is that the average size of kinetoplasts in the collapsed phase at 50 mM NaCl is significantly smaller than that at 100 mM NaCl, with mean R_g of 0.419 ± 0.042 μm and 0.494 ± 0.053 μm respectively (Welch's unpaired t test, $p < 0.0001$, Figure S7). This can be rationalized by envisioning that the local foci come together by the process of diffusion−collision,[64] and the packing is decided by the nature of collisions (reaction limited aggregation (RLA) vs diffusion limited aggregation (DLA)).[65] In the case of 50 mM NaCl, the potential barrier is higher (relatively less screening) and the mechanism of RLA is expected to be dominant. Hence, the degree of compaction in the collapsed phase is greater in 50 mM NaCl salt. This can be further explored in future experiments.

In conclusion, this work investigated the Ψ-phase transition of kinetoplasts. We found that kinetoplasts undergo a transition from the flat phase to the collapsed phase above a critical concentration of PEG, and this concentration is inversely correlated with the ionic strength of the system. Contrary to the linear DNA, the phase transition of kinetoplasts passes through a transition regime characterized by coexistence of a thermodynamically stable multipopulation of varying shapes and sizes. Molecular conformations in the multipopulation state are long-lived, which implies a rugged energy landscape and could be an intrinsic characteristic of 2D catenated networks. In the same way that Ψ-condensation of linear DNA has contributed significantly to the understanding

https://doi.org/10.1021/acsmacrolett.1c00463
ACS Macro Lett. 2021, 10, 1429−1435

of the conformational behavior of linear polymers in theta and poor solvents, as well as the packing of DNA in vivo, we believe that our study leads to a new understanding of the phase behavior of 2D catenated systems. We hope this work provokes future studies examining the role of topology in phase transitions of catenated polymers.

■ ASSOCIATED CONTENT

Supporting Information

The Supporting Information is available free of charge at https://pubs.acs.org/doi/10.1021/acsmacrolett.1c00463.

Details about experimental protocol, additional confocal images of kinetoplasts, data supporting the thermodynamic stability of the intermediate phase and the influence of YOYO-1 loading on the nature of phase transition, sketch of the postulated routes of phase transition, and a statistical test comparing the mean R_g in the collapsed phase under different salt conditions (PDF)

■ AUTHOR INFORMATION

Corresponding Author

Patrick S. Doyle − *Department of Chemical Engineering, Massachusetts Institute of Technology, Cambridge, Massachusetts 02139, United States; Harvard Medical School Initiative for RNA Medicine, Boston, Massachusetts 02215, United States;* orcid.org/0000-0003-2147-9172; Email: pdoyle@mit.edu

Authors

Indresh Yadav − *Department of Chemical Engineering, Massachusetts Institute of Technology, Cambridge, Massachusetts 02139, United States;* orcid.org/0000-0003-0060-1298

Dana Al Sulaiman − *Department of Chemical Engineering, Massachusetts Institute of Technology, Cambridge, Massachusetts 02139, United States*

Beatrice W. Soh − *Institute of Materials Research and Engineering, Singapore 138634, Singapore*

Complete contact information is available at: https://pubs.acs.org/10.1021/acsmacrolett.1c00463

Author Contributions

‡These authors contributed equally to this work.

Notes

The authors declare no competing financial interest.

■ ACKNOWLEDGMENTS

This project was funded by NSF Grant CBET-1936696. We thank Dr. Wendy Salmon of the W. M. Keck Facility for Biological Imaging at the Whitehead Institute for her support in confocal imaging.

■ REFERENCES

(1) Qiu, L. Y.; Bae, Y. H. Polymer Architecture and Drug Delivery. *Pharm. Res.* **2006**, *23* (1), 1−30.

(2) Zhu, X.; Zhou, Y.; Yan, D. Influence of Branching Architecture on Polymer Properties. *J. Polym. Sci., Part B: Polym. Phys.* **2011**, *49* (18), 1277−1286.

(3) Rauscher, P. M.; Rowan, S. J.; De Pablo, J. J. Topological Effects in Isolated Poly[n]Catenanes: Molecular Dynamics Simulations and Rouse Mode Analysis. *ACS Macro Lett.* **2018**, *7* (8), 938−943.

(4) Wulstein, D. M.; Regan, K. E.; Garamella, J.; McGorty, R. J.; Robertson-Anderson, R. M. Topology-Dependent Anomalous Dynamics of Ring and Linear DNA Are Sensitive to Cytoskeleton Crosslinking. *Sci. Adv.* **2019**, *5* (12), No. eaay5912.

(5) Smrek, J.; Garamella, J.; Robertson-Anderson, R.; Michieletto, D. Topological Tuning of DNA Mobility in Entangled Solutions of Supercoiled Plasmids. *Sci. Adv.* **2021**, *7* (20), No. eabf9260.

(6) Seiler, M. Hyperbranched Polymers: Phase Behavior and New Applications in the Field of Chemical Engineering. *Fluid Phase Equilib.* **2006**, *241* (1−2), 155−174.

(7) Schlüter, A. D.; Payamyar, P.; Öttinger, H. C. How the World Changes By Going from One- to Two-Dimensional Polymers in Solution. *Macromol. Rapid Commun.* **2016**, *37* (20), 1638−1650.

(8) Stupp, S. I.; Son, S.; Lin, H. C.; Li, L. S. Synthesis of Two-Dimensional Polymers. *Science* **1993**, *259* (5091), 59−63.

(9) Kim, K. O.; Choi, T. L. Synthesis of Rod-like Dendronized Polymers Containing G4 and G5 Ester Dendrons via Macromonomer Approach by Living ROMP. *ACS Macro Lett.* **2012**, *1* (4), 445−448.

(10) Colson, J. W.; Dichtel, W. R. Rationally Synthesized Two-Dimensional Polymers. *Nat. Chem.* **2013**, *5* (6), 453−465.

(11) Kissel, P.; Murray, D. J.; Wulftange, W. J.; Catalano, V. J.; King, B. T. A Nanoporous Two-Dimensional Polymer by Single-Crystal-to-Single-Crystal Photopolymerization. *Nat. Chem.* **2014**, *6* (9), 774−778.

(12) August, D. P.; Dryfe, R. A. W.; Haigh, S. J.; Kent, P. R. C.; Leigh, D. A.; Lemonnier, J. F.; Li, Z.; Muryn, C. A.; Palmer, L. I.; Song, Y.; Whitehead, G. F. S.; Young, R. J. Self-Assembly of a Layered Two-Dimensional Molecularly Woven Fabric. *Nature* **2020**, *588* (7838), 429−435.

(13) Mao, C.; Sun, W.; Seeman, N. C. Assembly of Borromean Rings from DNA. *Nature* **1997**, *386* (13), 137.

(14) Krajina, B. A.; Zhu, A.; Heilshorn, S. C.; Spakowitz, A. J. Active DNA Olympic Hydrogels Driven by Topoisomerase Activity. *Phys. Rev. Lett.* **2018**, *121* (14), 148001.

(15) Hart, L. F.; Hertzog, J. E.; Rauscher, P. M.; Rawe, B. W.; Tranquilli, M. M.; Rowan, S. J. Material Properties and Applications of Mechanically Interlocked Polymers. *Nat. Rev. Mater.* **2021**, *6* (June), 508−530.

(16) Simpson, L.; Berliner, J. Isolation of the Kinetoplast DNA of Leishmania Tarentohe in the Form of a Network. *J. Protozool.* **1974**, *21* (2), 382−393.

(17) Englund, P. T. The Replication of Kinetoplast DNA Networks in Crithidia Fasciculata. *Cell* **1978**, *14* (1), 157−168.

(18) Chen, J.; Rauch, C. A.; White, J. H.; Englund, P. T.; Cozzarelli, N. R. The Topology of the Kinetoplast DNA Network. *Cell* **1995**, *80* (1), 61−69.

(19) Michieletto, D.; Marenduzzo, D.; Orlandini, E. Is the Kinetoplast DNA a Percolating Network of Linked Rings at Its Critical Point? *Phys. Biol.* **2015**, *12* (3), 036001.

(20) Zang, Y.; Aoki, T.; Teraguchi, M.; Kaneko, T.; Ma, L.; Jia, H. Two-Dimensional and Related Polymers: Concepts, Synthesis, and Their Potential Application as Separation Membrane Materials. *Polym. Rev.* **2015**, *55* (1), 57−89.

(21) de Gennes, P.-G. *Scaling Concepts in Polymer Physics*; Cornell University Press: New York, 1979.

(22) Klotz, A. R.; Soh, B. W.; Doyle, P. S. Equilibrium Structure and Deformation Response of 2D Kinetoplast Sheets. *Proc. Natl. Acad. Sci. U. S. A.* **2020**, *117* (1), 121−127.

(23) Grosberg, A. Y. Human Bloodsucking Parasite in Service of Materials Science. *Proc. Natl. Acad. Sci. U. S. A.* **2020**, *117* (1), 18−20.

(24) Soh, B. W.; Doyle, P. S. Deformation Response of Catenated DNA Networks in a Planar Elongational Field. *ACS Macro Lett.* **2020**, *9* (7), 944−949.

(25) Soh, B. W.; Khorshid, A.; Al Sulaiman, D.; Doyle, P. S. Ionic Effects on the Equilibrium Conformation of Catenated DNA Networks. *Macromolecules* **2020**, *53* (19), 8502−8508.

(26) Soh, B. W.; Doyle, P. S. Equilibrium Conformation of Catenated DNA Networks in Slitlike Confinement. *ACS Macro Lett.* **2021**, *10*, 880−885.

(27) Wang, W.; Schlüter, A. D. Synthetic 2D Polymers: A Critical Perspective and a Look into the Future. *Macromol. Rapid Commun.* **2019**, *40* (1), 1−29.
(28) Ren, Y.; Yu, C.; Chen, Z.; Xu, Y. Two-Dimensional Polymer Nanosheets for Efficient Energy Storage and Conversion. *Nano Res.* **2021**, *14* (6), 2023−2036.
(29) Kantor, Y.; Nelson, D. R. Crumpling Transition in Polymerized Membranes. *Phys. Rev. Lett.* **1987**, *58* (26), 2774.
(30) Abraham, F. F.; Kardar, M. Folding and Unfolding Transitions in Tethered Membranes. *Science* **1991**, *252* (5004), 419.
(31) Wen, X.; Garland, C. W.; Hwa, T.; Kardar, M.; Kokufuta, E.; Li, Y.; Orkisz, M.; Tanaka, T. Crumpled and Collapsed Conformation in Graphite Oxide Membranes. *Nature* **1992**, *355* (6359), 426−428.
(32) Abraham, F. F.; Goulian, M. Diffraction from Polymerized Membranes: Flat vs. Crumpled. *Epl* **1992**, *19* (4), 293−296.
(33) Koltonow, A. R.; Luo, C.; Luo, J.; Huang, J. Graphene Oxide Sheets in Solvents: To Crumple or Not to Crumple? *ACS Omega* **2017**, *2* (11), 8005−8009.
(34) Wang, Y.; Wang, S.; Li, P.; Rajendran, S.; Xu, Z.; Liu, S.; Guo, F.; He, Y.; Li, Z.; Xu, Z.; Gao, C. Conformational Phase Map of Two-Dimensional Macromolecular Graphene Oxide in Solution. *Matter* **2020**, *3* (1), 230−245.
(35) Kapahnke, F.; Schmidt, U.; Heermann, D. W.; Weiss, M. Polymer Translocation through a Nanopore: The Effect of Solvent Conditions. *J. Chem. Phys.* **2010**, *132* (16), 164904.
(36) Lerman, L. S. Compact Form of DNA in Polymer Solutions. *Proc. Natl. Acad. Sci. U. S. A.* **1971**, *68* (8), 1886−1890.
(37) Minagawa, K.; Matsuzawa, Y.; Yoshikawa, K.; Khokhlov, A. R.; Doi, M. Direct Observation of the Coil-globule Transition in Dna Molecules. *Biopolymers* **1994**, *34* (4), 555−558.
(38) Vasilevskaya, V. V.; Khokhlov, A. R.; Matsuzawa, Y.; Yoshikawa, K. Collapse of Single DNA Molecule in Poly (Ethylene Glycol) Solutions. *J. Chem. Phys.* **1995**, *102* (16), 6595−6602.
(39) Ramos, J. E. B.; de Vries, R.; Ruggiero Neto, J. DNA ψ-Condensation and Reentrant Decondensation: Effect of the PEG Degree of Polymerization. *J. Phys. Chem. B* **2005**, *109* (49), 23661−23665.
(40) Kawakita, H.; Uneyama, T.; Kojima, M.; Morishima, K.; Masubuchi, Y.; Watanabe, H. Formation of Globules and Aggregates of DNA Chains in DNA/Polyethylene Glycol/Monovalent Salt Aqueous Solutions. *J. Chem. Phys.* **2009**, *131* (9), 094901.
(41) Miyoshi, D.; Sugimoto, N. Molecular Crowding Effects on Structure and Stability of DNA. *Biochimie* **2008**, *90* (7), 1040−1051.
(42) Xu, W.; Muller, S. J. Polymer-Monovalent Salt-Induced DNA Compaction Studied via Single-Molecule Microfluidic Trapping. *Lab Chip* **2012**, *12* (3), 647−651.
(43) Halperin, A.; Goldbart, P. M. Early Stages of Homopolymer Collapse. *Phys. Rev. E: Stat. Phys., Plasmas, Fluids, Relat. Interdiscip. Top.* **2000**, *61* (1), 565−573.
(44) Dobrynin, A. V.; Rubinstein, M. Theory of Polyelectrolytes in Solutions and at Surfaces. *Prog. Polym. Sci.* **2005**, *30* (11), 1049−1118.
(45) Lukeš, J.; Guilbride, D. L.; Votýpka, J.; Zíková, A.; Benne, R.; Englund, P. T. Kinetoplast DNA Network: Evolution of an Improbable Structure. *Eukaryot. Cell* **2002**, *1* (4), 495−502.
(46) Hsieh, C. C.; Balducci, A.; Doyle, P. S. An Experimental Study of DNA Rotational Relaxation Time in Nanoslits. *Macromolecules* **2007**, *40* (14), 5196−5205.
(47) Lifshitz, I. M.; Grosberg, A. Y.; Khokhlov, A. R. Some Problems of the Statistical Physics of Polymer Chains with Volume Interaction. *Rev. Mod. Phys.* **1978**, *50* (3), 683−713.
(48) Yaffe, N.; Rotem, D.; Soni, A.; Porath, D.; Shlomai, J. Direct Monitoring of the Stepwise Condensation of Kinetoplast DNA Networks. *Sci. Rep.* **2021**, *11* (1), 1−13.
(49) Khokhlov, A. R.; Takahashi, M.; Vasilevskaya, V. V. Large Discrete Transition in a Single DNA Molecule Appears Continuous in the Ensemble. *Phys. Rev. Lett.* **1996**, *76* (16), 3029−3031.
(50) Zinchenko, A. A.; Yoshikawa, K. Na+ Shows a Markedly Higher Potential than K+ in DNA Compaction in a Crowded Environment. *Biophys. J.* **2005**, *88* (6), 4118−4123.
(51) Xi, B.; Ran, S. Formation of DNA Pearl-Necklace Structures on Mica Surface Governed by Kinetics and Thermodynamics. *J. Polym. Sci., Part B: Polym. Phys.* **2017**, *55*, 971−979.
(52) Ueda, M.; Yoshikawa, K. Phase Transition and Phase Segregation in a Single Double-Stranded Dna Molecule. *Phys. Rev. Lett.* **1996**, *77* (10), 2133−2136.
(53) Yoshikawa, K.; Matsuzawa, Y. Nucleation and Growth in Single DNA Molecules. *J. Am. Chem. Soc.* **1996**, *118* (4), 929−930.
(54) Zinchenko, A. A.; Sergeyev, V. G.; Murata, S.; Yoshikawa, K. Controlling the Intrachain Segregation on a Single DNA Molecule. *J. Am. Chem. Soc.* **2003**, *125* (15), 4414−4415.
(55) Takagi, S.; Tsumoto, K.; Yoshikawa, K. Intra-Molecular Phase Segregation in a Single Polyelectrolyte Chain. *J. Chem. Phys.* **2001**, *114* (15), 6942−6949.
(56) Günther, K.; Mertig, M.; Seidel, R. Mechanical and Structural Properties of YOYO-1 Complexed DNA. *Nucleic Acids Res.* **2010**, *38* (19), 6526−6532.
(57) Kundukad, B.; Yan, J.; Doyle, P. S. Effect of YOYO-1 on the Mechanical Properties of DNA. *Soft Matter* **2014**, *2014* (48), 9721−9728.
(58) De Vries, R. Flexible Polymer-Induced Condensation and Bundle Formation of DNA and F-Actin Filaments. *Biophys. J.* **2001**, *80* (3), 1186−1194.
(59) Krotova, M. K.; Vasilevskaya, V. V.; Makita, N.; Yoshikawa, K.; Khokhlov, A. R. DNA Compaction in a Crowded Environment with Negatively Charged Proteins. *Phys. Rev. Lett.* **2010**, *105* (12), 1−4.
(60) Zinchenko, A.; Berezhnoy, N. V.; Chen, Q.; Nordenskiöld, L. Compaction of Single-Molecule Megabase-Long Chromatin under the Influence of Macromolecular Crowding. *Biophys. J.* **2018**, *114* (10), 2326−2335.
(61) Bryngelson, J. D.; Wolynes, P. G. Spin Glasses and the Statistical Mechanics of Protein Folding. *Proc. Natl. Acad. Sci. U. S. A.* **1987**, *84* (21), 7524−7528.
(62) Onuchic, J. N.; Luthey-Schulten, Z.; Wolynes, P. G. Theory of Protein Folding: The Energy Landscape Perspective. *Annu. Rev. Phys. Chem.* **1997**, *48* (1), 545−600.
(63) Asakura, S.; Oosawa, F. On Interaction between Two Bodies Immersed in a Solution of Macromolecules. *J. Chem. Phys.* **1954**, *22* (7), 1255−1256.
(64) Karplus, M.; Weaver, D. L. Protein-Folding Dynamics. *Nature* **1976**, *260* (1), 404−406.
(65) Weitz, D. A.; Huang, J. S.; Lin, M. Y.; Sung, J. Limits of the Fractal Dimension for Irreversible Kinetic Aggregation of Gold Colloids. *Phys. Rev. Lett.* **1985**, *54* (13), 1416−1419.

https://doi.org/10.1021/acsmacrolett.1c00463
ACS Macro Lett. 2021, 10, 1429−1435